Journal of the European Ceramic Society **9** (1992) 323–334

Crack Closure Forces in Ceramics: Characterization and Formation

Jürgen Rödel

Advanced Ceramics Group, Technische Universität Hamburg–Harburg, D-2100 Hamburg 90, FRG

(Received 25 June 1991; accepted 12 August 1991)

Abstract

In-situ crack propagation studies using the scanning electron microscope (SEM) on seven materials are used to define three general categories for crack bridging elements: intact (elastic) bridges, frictionally sliding (plastic) bridges and mechanically interlocked (elastic–plastic) bridges. A number of examples are provided, some including sequences detailing bridge formation and bridge evolution. Failure modes of all these restraining elements, their interrelations and synergistic effects are discussed.

A simple fracture mechanics model attempts to provide the criteria for bridge formation. The relevant microstructural parameters are grain size and shape, intra- or intercrystalline fracture energy, residual stress and Young's modulus.

In-situ Rissausbreitung an sieben verschiedenen Materialien im Rasterelektronenmikroskop (REM) dient als Grundlage um drei allgemeine Klassen von Elementen die der Rissüberbrückung dienen, zu definieren. Diese sind: intakte (elastische) Brücken, Reibungsbrücken (plastische Brücken) und mechanisch verhakte (elastisch–plastische) Brücken. Eine Anzahl von Beispielen, z.T. Folgen, erläutern Brückenbildung und Brückenentwicklung.

Ein einfaches Modell aus der Bruchmechanik versucht, Kriterien zur Brückenbildung zu geben. Als entscheidende Gefügeparameter werden Korngrösse und Kornform, intra- oder interkristalline Bruchenergie, Restspannungen und E-modul identifiziert.

Sur la base d'études in-situ de propagation de fissures, réalisées par microscopie électronique à balayage (MEB) sur sept matériaux, on définit trois grandes catégories d'éléments pour le pontage de fissure: les ponts intacts (élastiques), le ponts (plastiques) glissant par frottement et les ponts (élastiques–plastiques) mécaniquement enchevêtrés. De nombreux exemples sont fournis, certains incluant des séquences détaillant la formation et l'évolution des ponts. On discute des modes de rupture de tous ces éléments retardateurs, de leurs inter-relations et de leurs effets synergétiques.

Un modèle simple de mécanique de la rupture a pour ambition de fournir les critères responsables de la formation d'un pont. Les paramètres microstructuraux pertinents sont: la taille et le forme des grains, l'énergie de rupture intra- ou intercristalline, la contrainte résiduelle et le module d'Young.

1 Introduction

Ceramic materials still find only limited application because of their brittleness. A sound approach to increase the fracture toughness in these materials is therefore the delocalization of the fracture process. This allows a participation of the crack interfaces and the surrounding areas in the energy absorption process and thereby shielding of the crack tip from the externally applied load. These mechanisms are divided into dilation (transformation toughening[1] and microcrack toughening[2]) and crack bridging[3–6] (use of crack closure forces to limit a further opening of the crack). Both mechanisms lead to *R*-curve behaviour, an increase in crack resistance with increasing crack length. The focus here will be on crack closure forces with sole emphasis on brittle restraining elements.

To avoid confusion some simple definitions are given here.

Crack closure force (also crack interface traction)—closure traction which is applied perpendicular to the crack interfaces, thereby reducing the crack opening displacement

Journal of the European Ceramic Society 0955-2219/92/$5.00

(COD). Closure forces can be combined (for restrictions see discussion by Smith[7]) and can be taken as a smeared out closure stress (p) as a function of crack opening ($2u$). They are then represented as $p(u)$ function.

Bridge (also bridging element, restraining element)—any microstructural element which provides a closure force in the crack wake.

Primary crack (also main crack)—crack system providing continuous (at least one-dimensional) link between crack mouth and crack tip, not necessarily continuous in two dimensions.

Secondary crack—connected to primary crack; opening of secondary crack is derived from closure force across primary crack. Secondary cracks close therefore when closure force subsides.

Microcrack—small crack (with respect to the microstructure), not usually connected to primary crack. Opening arises from residual stress, therefore persistent.

While a number of discrete bridging elements have been studied in detail, e.g. fibres,[8] whiskers,[6] particular grain configurations,[9] a more general picture has not yet emerged. The attempt here is therefore to step back and develop a fundamental characterization and classification of crack closure forces in different types of materials which could include fibres, whiskers, elongated grains, etc. The hope then is to give general guidelines to the processing community to help in the quest for tougher materials.

The study was conducted in two parts. Firstly, an in-depth characterization of bridge configurations: what kind of bridges can be found, in what situation do they occur, how is energy absorbed and how do they fail. For this part an in-situ straining stage,[10,11] custom designed for the SEM, was used. Secondly, a simplistic theoretical analysis is given describing the formation of closure forces. This model describes generation of a single microcrack at the crack tip and is based on detailed crack propagation studies. Four classes of materials were investigated:

(a) Materials with a modest thermal expansion anisotropy (two aluminas);
(b) materials containing strong reinforcements (two silicon carbide whisker-reinforced aluminas);
(c) materials with strong internal residual stresses (two Al_2TiO_5/Al_2O_3 composites);
(d) a more complex, metal- and particulate-reinforced alumina-based composite (SiC/Al/Al_2O_3).

2 Experimental

All microstructural observations were obtained with an in-situ custom-designed straining stage built into an SEM chamber.[10,11] Extension of a piezoelectric translator delivers a finely tuneable load (measured through a load cell) to the specimen. Crack propagation is quasi-static and recorded on videotape with intermittent periods of static loading to allow for closer observation and micrographic recording. Details concerning the design of the fracture stage can be found elsewhere.[11] Similar devices for different crack geometries are also described by Frei & Grathwohl.[12] All micrographs shown are taken from specimens held at $\approx 95\%$ of the equilibrium load for crack extension.

Crack–microstructure interactions were recorded using compact tension specimens. This sample geometry offers the advantage of extensive stable crack propagation. A large sample area is therefore intersected by the primary crack with an accompanying large number of microstructural sites being activated as elements applying closure forces in the crack wake. Observations were specifically made at the crack tip to determine how and when bridges are formed but also in the crack wake to observe evolution of already identified bridging elements. Cracks are driven in either half-chevron geometry[10] or in a regime with constant sample thickness.

Bridging elements are characterized by their distance to the crack tip, x, and their accompanying local crack opening displacement, $2u$. The prime goal was the observation of microstructural elements close to the crack tip ($x < 1$ mm) in a regime where penny-shaped cracks might still be in a stable mode of crack propagation. Compact tension specimens are tempting, since bridges far behind the crack tip ($x > 1$ mm) can be characterized, yet these observations are somewhat irrelevant as cracks originating from surface flaws experience closure forces from these bridges only while they are already in an unstable mode of crack propagation. The local crack opening, $2u$, is the relevant parameter which enters into the stress displacement function, $p(u)$. Knowledge of the $p(u)$ relationship allows computation of a geometry- and stress-field invariant R-curve as a function of crack opening ($R(u)$).[10]

The materials chosen for this study were:

—a hot-pressed alumina (average grain size, $\bar{G} = 11\ \mu$m);
—a commercial alumina ($\bar{G} = 35\ \mu$m, Vistal grade alumina, Coors Ceramics, Colorado, USA);
—a hot-pressed SiC_w/Al_2O_3 with 30 vol.% large

SiC whiskers (TWS-400, Tokai Carbon Ltd, Japan), referred to as $30SiC_w/Al_2O_3$;
—a hot-pressed SiC_w/Al_2O_3 with 20 vol.% small SiC whiskers (TWS-100, Tokai Carbon Ltd, Japan), referred to as $20SiC_w/Al_2O_3$;
—an Al_2TiO_5/Al_2O_3 composite[13] (containing 20 vol.% Al_2TiO_5) with $\bar{G} \approx 6\,\mu m$ for Al_2O_3 and $\bar{G} \approx 3\,\mu m$ for the Al_2TiO_5;
—an Al_2TiO_5/Al_2O_3 composite[14] (as above but also containing large ($\bar{G} \approx 25\,\mu m$) alumina grains);
—an $Al/Al_2O_3/SiC$ composite material (Alanx FGS, Alanx Products L.P., Newark, DE, USA).

3 Characterization of Crack Closure Forces

Again a broad view is chosen, where results are presented irrespective of material investigated. Microscopical observations are classified in terms of bridge categories. General guidelines are sought and will be discussed.

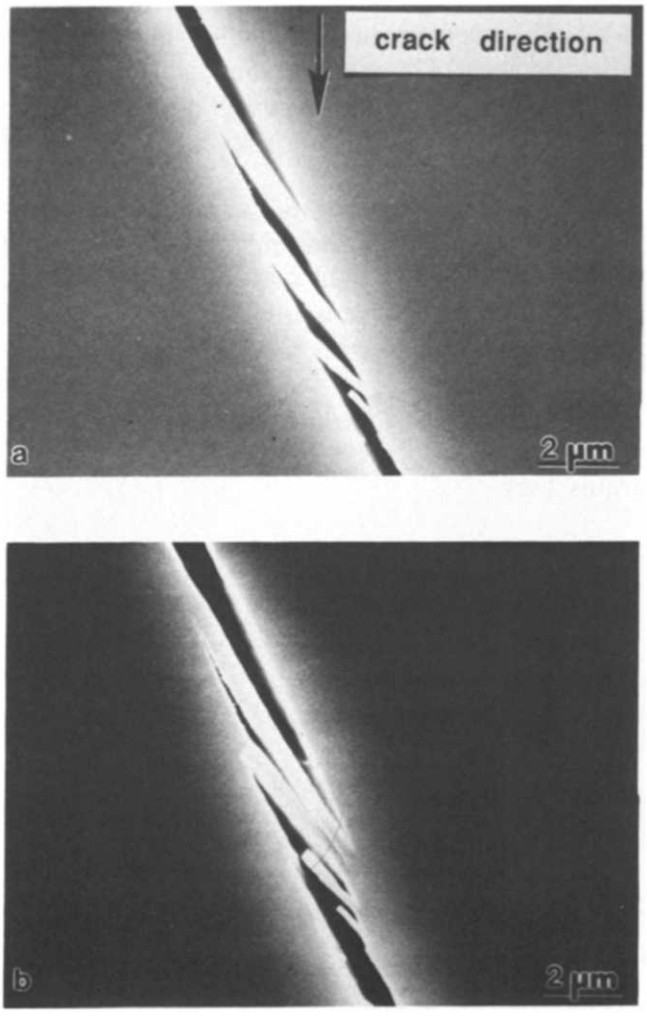

Fig. 1. Evolution of intact micro-bridges in an α-SiC grain embedded in an Al/Al_2O_3 matrix; the direction of crack propagation is from top to bottom in both micrographs: (a) x (distance from the crack tip) = 410 μm, $2u$ (total crack opening) = 540 nm; (b) x = 530 μm, $2u$ = 750 nm.

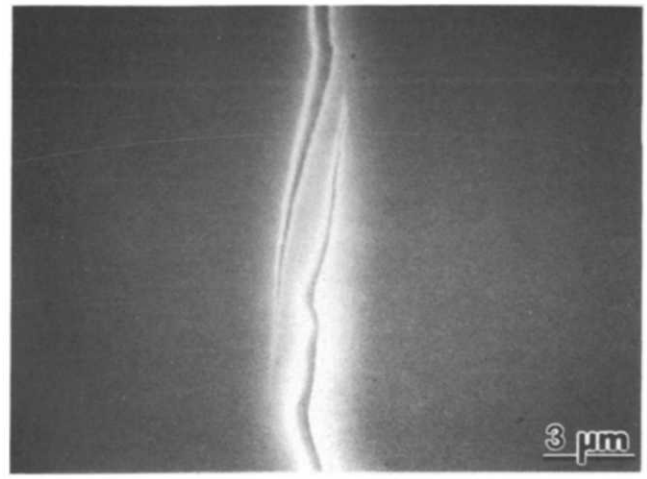

Fig. 2. Unbroken micro-bridge (or 'handshake') in Al_2O_3: $x \approx$ 700 μm, $2u \approx$ 600 nm.

Based on observations in the SEM three bridge categories are established: intact bridge, frictionally sliding bridge and mechanically interlocked bridge. A select number of examples are given, together with discussion of salient features of the three types.

3.1 Intact bridge

This type of restraining element relies on intact, unbroken microstructural elements.

Figure 1 shows the evolution of intact micro-bridges in an α-SiC grain (grain size ≈ 30 μm) embedded in an Al_2O_3–Al matrix. A term might be borrowed from the Geological Society[15] and this crack called a 'right-stepping crack', since the crack shifted about 0·5 μm to the right during crack advancement, thereby creating each of the four restraining elements. In Fig. 1(a) only one bridge is broken, while only one remains intact in Fig. 1(b).

Figure 2 shows an unbroken micro-bridge in the commercial alumina ($\bar{G} = 35\,\mu m$). A very picturesque description of this type of reinforcement is 'handshake'. Figure 3 shows an intact ligament (Fig. 3(a)) as it fails (breaks) and simultaneously transforms into a frictionally sliding bridge (Fig. 3(b)). The images are taken from the commercial alumina investigated.

Figure 4 is a micrograph of a bridging SiC whisker close to the crack tip in a $30SiC_w/Al_2O_3$ matrix. Debonding did not occur close to the interface but in the alumina, about 100 nm away from the interface itself. This particular whisker broke at a total COD of 300 nm, when situated 120 μm behind the crack tip.

Figure 5 shows three intact whisker reinforcements ($30SiC_w/Al_2O_3$) closely lined up. The very

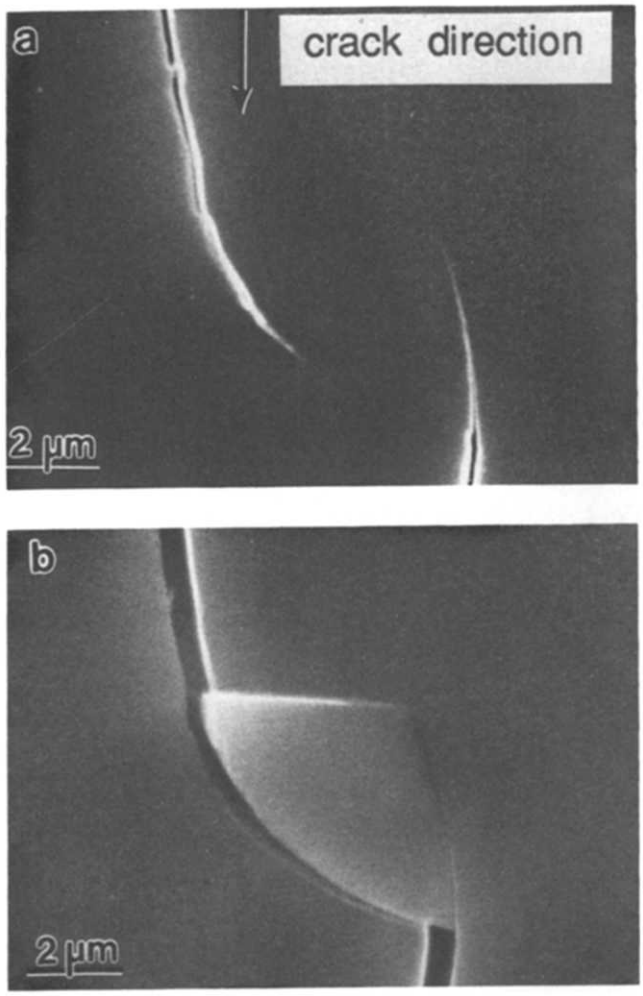

Fig. 3. In the commercial alumina (a) an intact bridge transforms into (b) a frictionally sliding bridge: (a) $x = 170\,\mu m$, $2u = 140\,nm$; (b) $x = 740\,\mu m$, $2u = 560\,nm$.

peculiar whisker shape might have aided bridge formation. In Fig. 6 two multi-grain intact ligaments are set up in an Al_2TiO_5/Al_2O_3 composite.

Intact bridges occur in different sizes; the micro-bridges (Figs 1 and 2) are of a ligament width of $<1\,\mu m$, which is much smaller than the grain size.

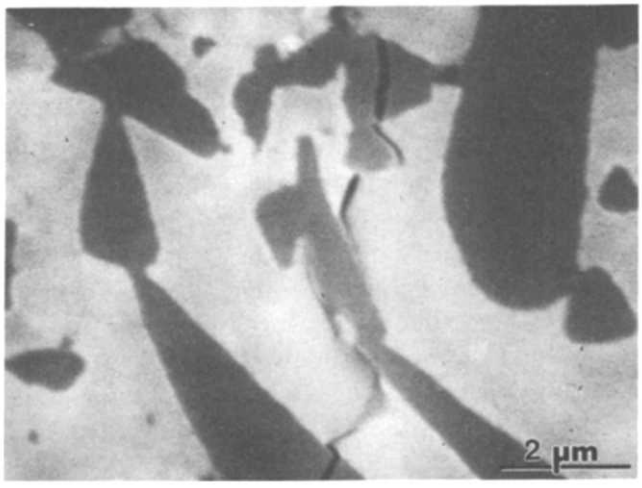

Fig. 4. Unbroken whisker provides restraining element in a $30SiC_w/Al_2O_3$ composite: $x = 10\,\mu m$, $2u = 80\,nm$.

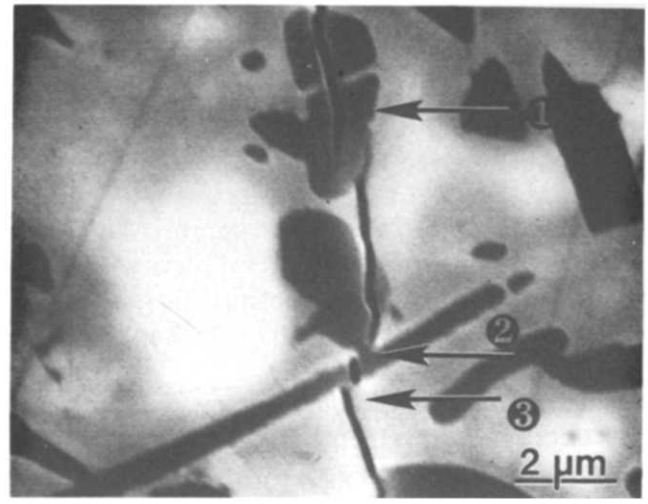

Fig. 5. Three intact SiC whisker elements in a $20SiC_w/Al_2O_3$ composite: $x = 40\,\mu m$, $2u = 140\,nm$.

These bridges therefore show transgranular failure. Restraining elements as in Fig. 1 have not been observed before, which is understandable, since it is very hard to detect them by optical microscopy alone. Their deformation behaviour (Fig. 1) allows the expectation of huge stresses and strains along the ligament (which, however, does not necessarily translate into a large closure stress perpendicular to the crack interfaces).

Bridges as in Fig. 3 might arise from partly intergranular, partly intragranular failure and are in the size range of the grain size. Reinforcements as seen in Figs 4 and 5 are mainly determined by the scale of the second phase. Bridging on a scale larger than the grain size[13] as in Fig. 6 involves intergranular failure and leads to unbroken reinforcements with ligaments several grains wide and tens of grains long.

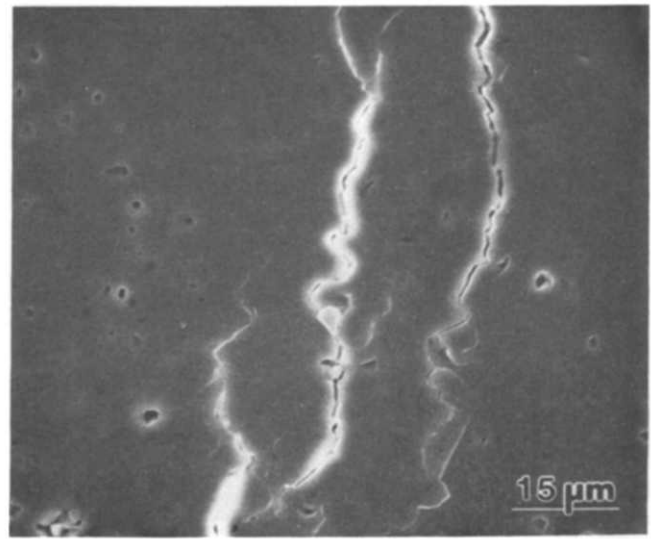

Fig. 6. Intact multi-grain ligaments in Al_2TiO_5/Al_2O_3 composite: $x \approx 700\,\mu m$, $2u \approx 1000\,nm$.

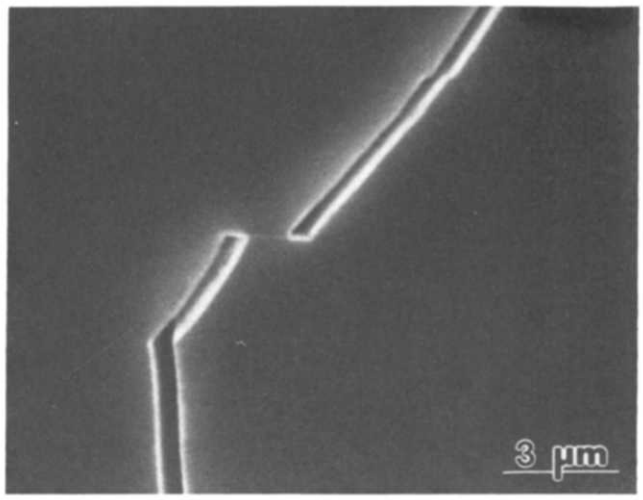

Fig. 7. Frictionally sliding bridge in commercial alumina: $x = 290\,\mu m$, $2u = 450$ nm.

This type of reinforcement is found particularly close to the crack tip (where closure forces weight in strongest[16]), but—as was demonstrated—are effective in cracks with CODs of about $0{\cdot}5\,\mu m$, which translates (depending on material, crack geometry, etc.) into cracks $\approx 0{\cdot}5$ mm long.

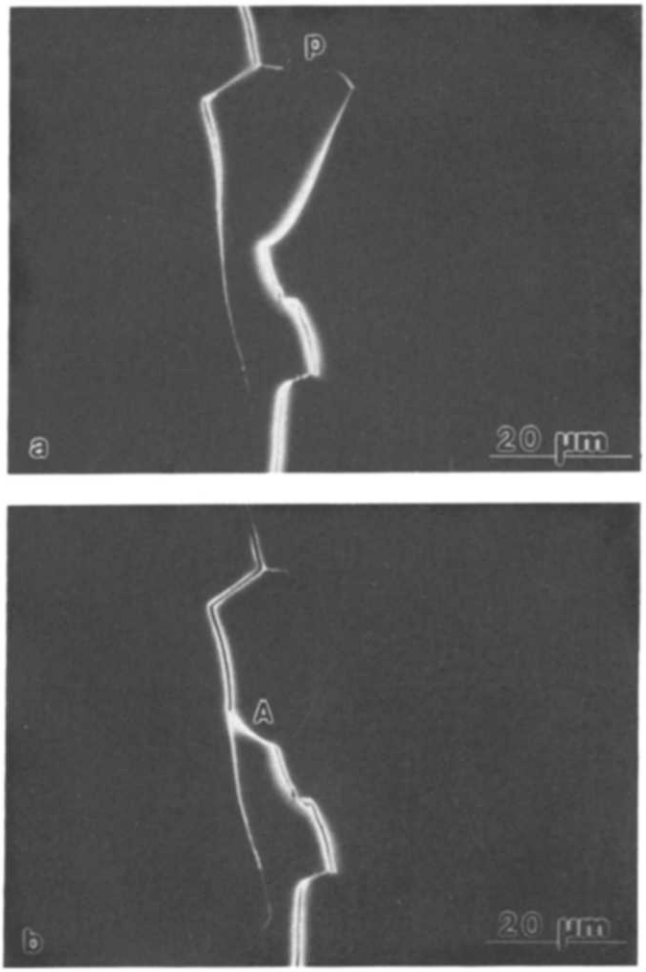

Fig. 8. Frictionally sliding bridge (a) breaks as shown in (b) in a commercial alumina: (a) $x = 880\,\mu m$, $2u \approx 750$ nm; (b) $x = 1080\,\mu m$, $2u \approx 900$ nm.

3.2 Frictionally sliding bridge

This restraining element relies on an element of friction which transforms a stress parallel to the general crack direction into a stress normal to the crack direction (closure stress).

In Fig. 7 the primary crack shifted right and left an almost invisible crack segment perpendicular to the crack direction. Repeated sliding with resultant abrasion[17] allowed verification that the crack interfaces were indeed in contact while sliding across each other.

A frictional element at point P in Fig. 8(a) is released by connecting a secondary crack at point A with the main crack (Fig. 8(b)). The poor visibility of the crack at P gives an indication of the possible existence of a frictionally sliding bridge. The fact that the crack is redirected (presumably to release a closure stress) is good evidence for the presence of the restraining element nearby.

Static micrographic observations of bridging elements alone appear insufficient to verify the existence of a frictionally sliding bridge. Further evidence, like debris accumulation or crack redirection from in-situ observations, is therefore very

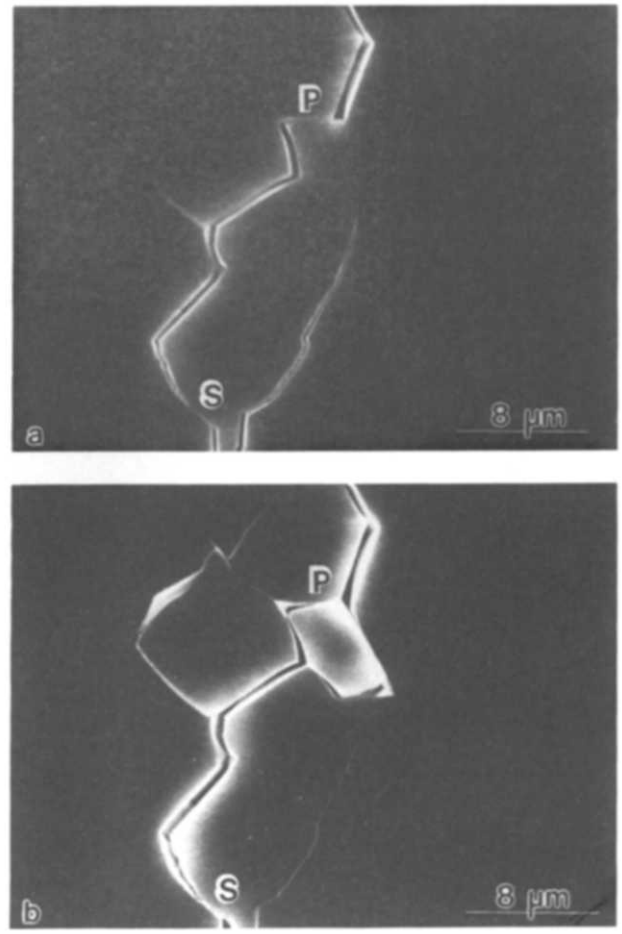

Fig. 9. Mechanically interlocking bridge at P and frictionally sliding bridge at S in hot-pressed alumina: (a) $x = 600\,\mu m$, $2u \approx 500$ nm; (b) $x = 1190\,\mu m$, $2u \approx 860$ nm.

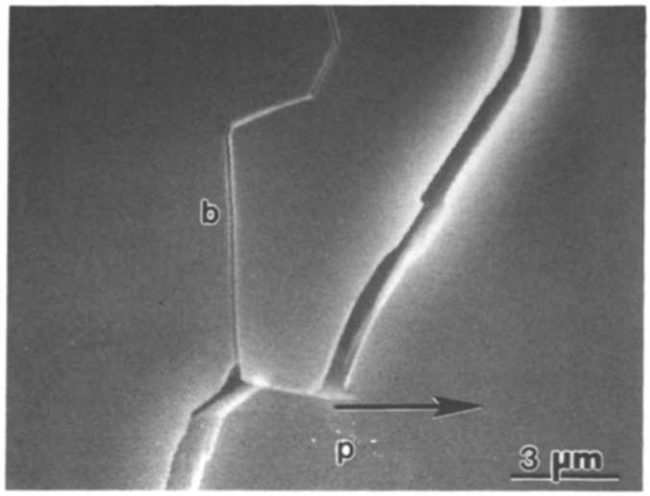

Fig. 10. Mechanically interlocking grain applies closure force at P in hot-pressed alumina, thereby pulling ligament to the right (arrow) and opening secondary crack b: $x = 810\,\mu m$, $2u = 600\,nm$.

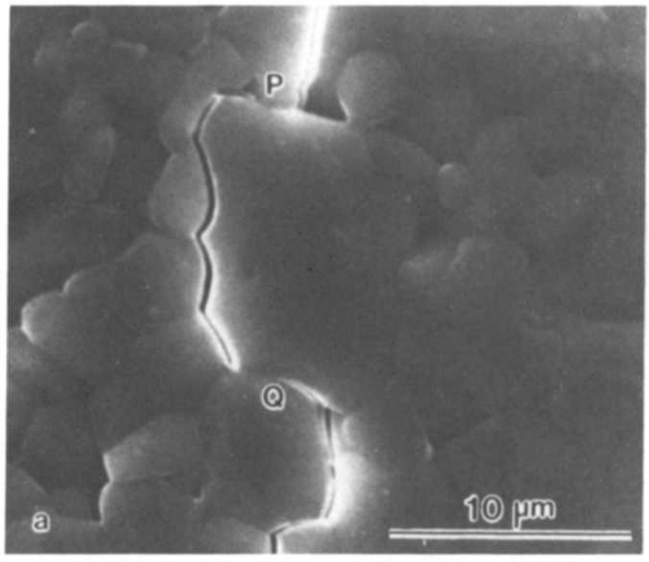

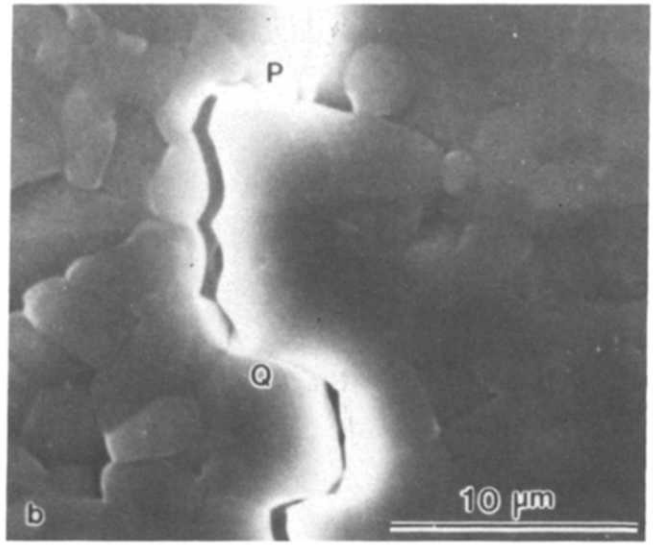

Fig. 11. Large alumina grain is mechanically interlocked with bridging tractions at P and Q in Al_2TiO_5/Al_2O_3 composite: (a) $x = 110\,\mu m$, $2u = 200\,nm$; (b) $x = 370\,\mu m$, $2u = 600\,nm$.

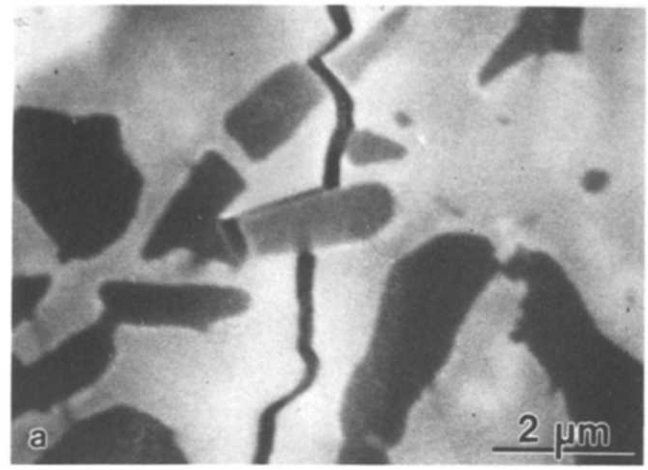

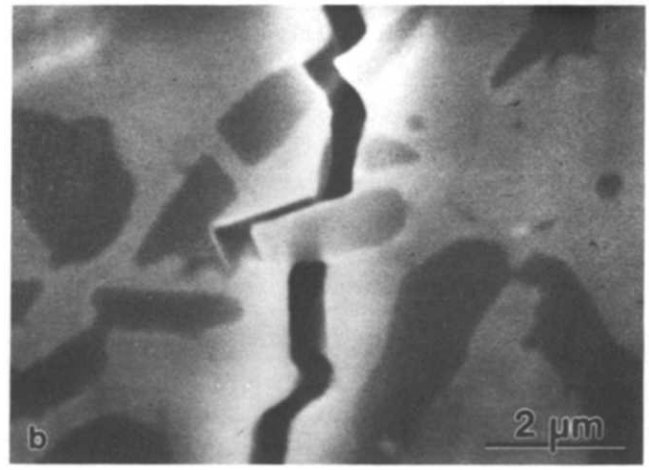

Fig. 12. Whisker pull-out in $30SiC_w/Al_2O_3$: (a) $x = 80\,\mu m$, $2u = 250\,nm$; (b) $x = 170\,\mu m$, $2u = 500\,nm$.

helpful. This type of restraining element can occur in all possible geometries but embodies usually one segment of the crack interfaces which lies close to perpendicular to the crack direction.

3.3 Mechanically interlocking bridge

Here a microstructural element is considered, which—although broken—remains wedged and applies a restraint to a further increase of the local crack opening displacement. This occurs at positions where a crack segment forms an acute angle with the crack plane (in other words, the crack retracted for a short distance).

A mechanically interlocking grain appears in Fig. 9(a) at point P. To reduce the restraint (Fig. 9(b)), it tries to rotate out of its socket, but also causes secondary cracking (note also frictionally sliding bridge at point S). A mechanically interlocking grain can be seen as a cantilever in Fig. 10 which, if stressed at point P by a closure force, will lead to a bending of the grain segment (arrow), visible through the opening of the secondary crack b.

The primary crack appears to retract at P, leading

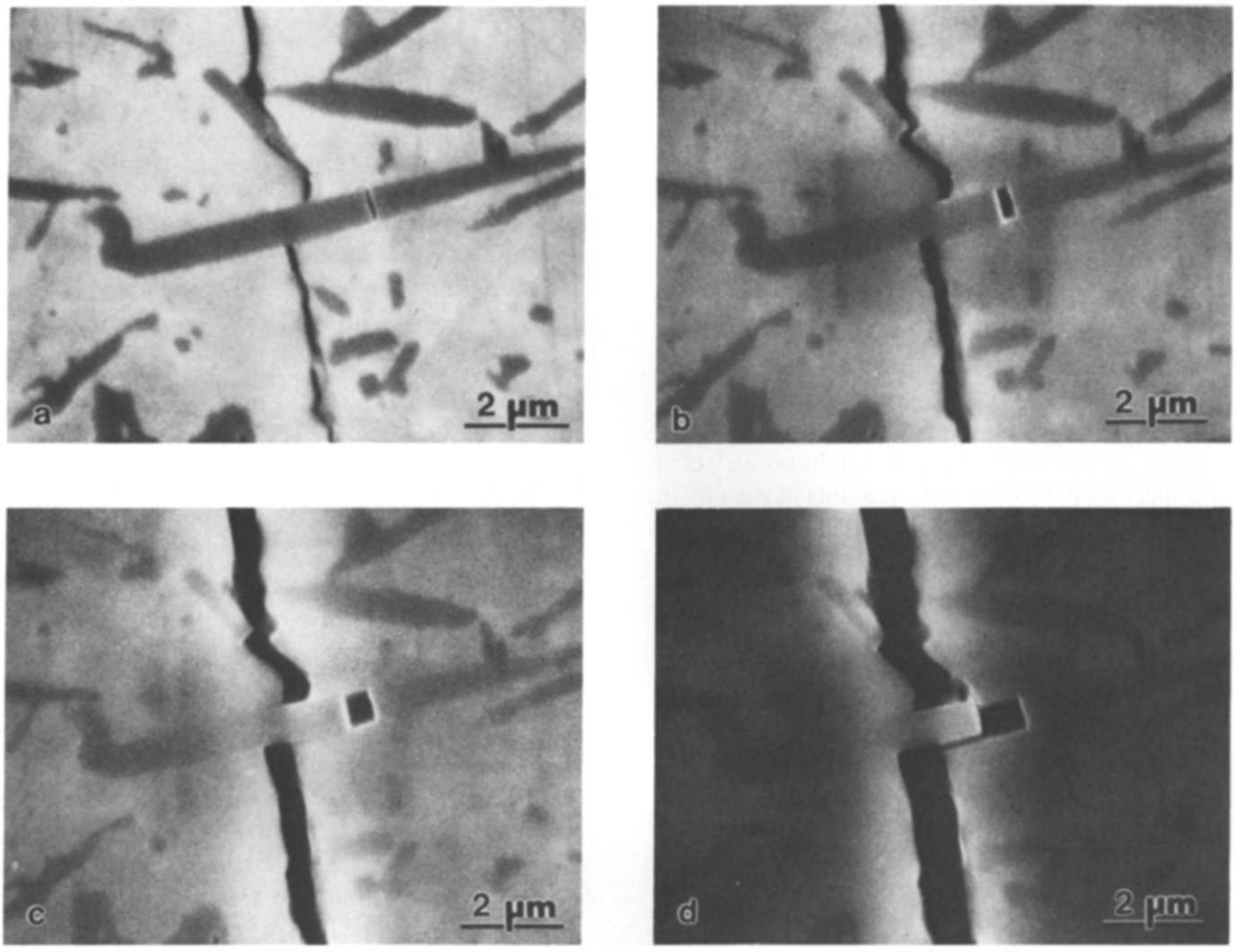

Fig. 13. Whisker pull-out in $20SiC_w/Al_2O_3$: (a) $x = 100\,\mu m$, $2u = 200\,nm$; (b) $x = 110\,\mu m$, $2u = 400\,nm$; (c) $x = 330\,\mu m$, $2u = 570\,nm$; (d) $x = 830\,\mu m$, $2u = 860\,nm$.

to mechanical interlocking of a large alumina grain in Fig. 11(a). Surface roughness at Q leads to additional mechanical restraint. Increased COD in Fig. 11(b) highlights critical contact points P and Q. A whisker in $30SiC_w/Al_2O_3$ is shown in Fig. 12 slightly inclined to the applied stress axis (Fig. 12(a)), thereby providing a mechanical restraint to pull-out, which has still not completely subsided in Fig. 12(b).

The case of whisker pull-out in Fig. 13 is similar to the description in Fig. 12. In distinction, the whisker angle to the crack plane is smaller, the restraining force is thereby higher (Fig. 13(a)–(c)), which leads to fracture of the restraining alumina matrix in Fig. 13(d) before the whisker has pulled out completely.

Mechanical interlocking occurs where (particularly elongated) microstructural elements are wedged and apply a mechanical restraint to pull-out. Stress release was seen to occur through either ligament rotation or fracture of the restraining matrix. Ligament fracture may also be possible.

4 Formation of Crack Closure Forces

An understanding of how restraining elements are set up is a key element in the attempt of tailoring microstructure aimed at producing tougher ceramics.

Bridge formation is governed by events occurring at the crack tip and is influenced by microstructural parameters influencing the crack path. Crack propagation itself is discontinuous with intermittent jumps equivalent to 1–100 grain lengths. Crack arrest can in some cases be related to strong reinforcements[18] or might be connected to compressive zones. These crack arrest sites might serve—after corresponding crack translation—as bridging elements, manifesting themselves in the discrete and bumpy nature of the *R*-curve. Other smaller bridging elements are set up without necessarily any crack arrest occurring at that particular site.

In focusing on the repropagation step (and

thereby the selection of crack path, in-situ observations recorded during the experiments performed in the SEM chamber are used. Quite frequently, particularly noticeable in the alumina materials, in Al_2TiO_5/Al_2O_3 and SiC_w/Al_2O_3, crack propagation occurs in two steps: (a) opening of a microcrack ahead of the crack tip and (b) joining of the microcrack to the primary crack (which could be restricted to the subsurface area, giving an elastic bridge at the surface). This step is distinct from deflection, where the crack remains continuous but changes direction on encountering a suitable reinforcement. Both events are governed by the same microstructural parameters. Since recent focus has been on the later step (fibre debonding,[8] etc.) while microscopical observation points at least to an equal degree to the first event, the opening of a microfacet in front of the crack tip is modelled and the characteristics under which a bridge is formed are given. This model is related to the known microcracking model,[19,20] a consequence which will be discussed.

Let us assume a crack tip in a microstructure as given in Fig. 14. Although the schematic diagram represents a case of intergranular fracture, the argument can be expanded to intragranular fracture as well. Take the event where crack translation occurs by either first opening a microfacet **a** or **d** with **b** and **c** remaining closed during that step. An opening of facet **a** with facet **b** opening subsequently would lead to a mechanically interlocked bridge, an elastic bridge if **b** does not open. An opening of facet **d** would not lead to a local crack retraction and therefore would not favour bridge formation.

The condition, in general terms, for a distinct microcrack source (which might see a local stress field, σ_{res}) to open under the local crack tip stress field, $\sigma(r)$, is given by[21]

$$T_0 = \frac{Y}{\sqrt{c}} \int_0^c \frac{[\sigma(r) + \sigma_{res}]r\,dr}{\sqrt{c^2 - r^2}} \qquad (1)$$

where T_0 is the grain boundary toughness (alternatively an intragranular fracture toughness), Y is a geometrical parameter determined by the crack shape, c is the length of a grain boundary defect, taken as a fixed fraction of the grain boundary facet length,[22] and r is the distance to the crack tip. Equation (1) is equally valid for microfacet **a** and **d**, and might be also written with subscripts **a** or **d**. Inspecting each of the microstructural parameters given in eqn (1) in turn, and if all other parameters for both cases (**a** or **d**) are assumed to be equal, then the opening of a microcrack at **a** (always in comparison to **d**) is favoured if:

(a) The grain facet at **a** is larger, leading to a larger value for c.
(b) The grain shape at **a** leads to a larger crack parameter Y.
(c) A smaller grain boundary toughness T_0 at **a** obtains.
(d) The residual stress term, σ_{res}, is larger at **a**.
(e) $\sigma(r)$ is larger at **a**, which occurs if **a** is closer to the crack tip than **d** (trivial), or if a stress field asymmetry occurs.

In this later case a mixed mode induces a disruption of the crack plane (seen as a local deflection) in order to seek a mode II (or III) = 0 criterion.[23] This can arise through a difference in Young's moduli (different phases) in the region in front of the crack tip. A second possibility obtains when the bridging zone itself (e.g. through geometrical interlocking and pull-out) creates a local mode II or III.

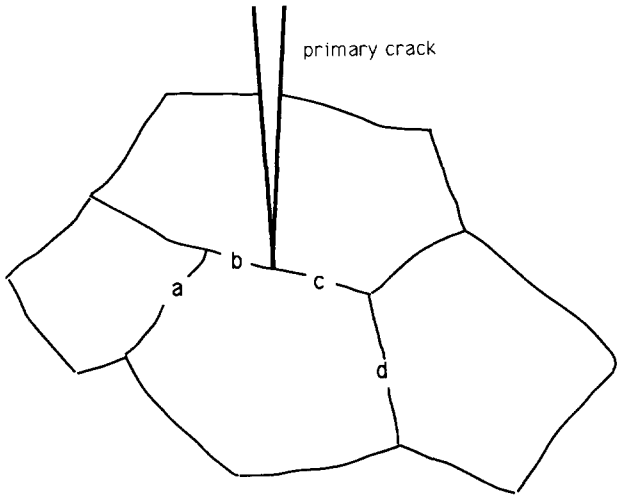

Fig. 14. Schematic diagram for bridge formation model. Creation of microcrack at either **a** or **d** ahead of the crack tip is considered. Facets **b** and **c** are assumed closed.

5 Discussion

5.1 Characterization of closure forces

A general classification scheme for closure forces has been presented. Intact bridges, frictionally sliding bridges and mechanically interlocking bridges (see Fig. 15) can be distinguished. Comparable attempts to shed some light on the various distinct closure force mechanisms are rarely found in the literature. Swanson[15] in his work on alumina and glass ceramics found two bridge categories: (a) frictional or geometrical interlocking and (b) ligamentary bridging by intact islands. Vekinis *et al.*[24] propose a similar classification scheme as presented here for

alumina with elastic bridges, frictionally sliding bridges and rotation of an angled bridging grain against restraining material. The latter is exemplified in Fig. 9, with closure force at P, but is viewed here only as a subcategory of the mechanically interlocked bridge. This restraining element might fail through rotation, cracking of the matrix (also in Fig. 9, with closure force at P, or Fig. 13) or even failure of the restraining element.

If attention is focused on intact bridges only (Fig. 15(a)), further subcategories depending either on bridge size or fracture path can be found. Microbridges, for example, exhibit transgranular failure mode with restraining elements much smaller than the grain size (Figs 1 and 2). Bridges of a size comparable to the grain size can show inter- or intragranular fracture (Figs 3 and 4) and multi-grain ligaments usually exhibit intergranular fracture (Fig. 6). A more mechanistic classification of intact bridges, however, distinguishes between restraining elements with fixed or no (Fig. 15(a)) or continued debonding (Fig. 15(b)). Intact bridges are essentially elastic in their deformation behaviour (or spring-like[25]). Therefore intact reinforcement is considered to be synonymous with elastic reinforcement. The $p(u)$ function is rising linearly, except for the case where continued debonding occurs and the compliance of the element changes with the local crack opening. Then the terminology elastic (no permanent deformation) does not strictly hold, since the debonding mechanism is not completely reversible. Nevertheless, the essentially elastic deformation implies complete resistance against cyclic loading: energy is not dissipated during loading (as in frictionally sliding bridges) but simply stored. A small degree of friction is only embodied in an elastic bridge if no concurrent bending moment is applied and the bridge pulls out of its socket perpendicular to the crack plane. Elastic restraining elements occur primarily close to the crack tip (but can be effective up to CODs of about 500 nm; see Fig. 1, etc.). They fail catastrophically under release of acoustic energy with the closure force either dropping to zero or transform into a bridge of one of the two other categories, thereby retaining part of the crack interface traction. Their existence in whisker-reinforced materials has been documented using SEM and TEM.[26] Vekinis *et al.*[24] observed elastic bridges in alumina, but only with small COD ($2u <$ 100 nm).

The frictionally sliding bridge has been recognized and discussed by various groups.[5,15,24,27] The friction coefficient serves as a proportionality constant required to transform stresses parallel to

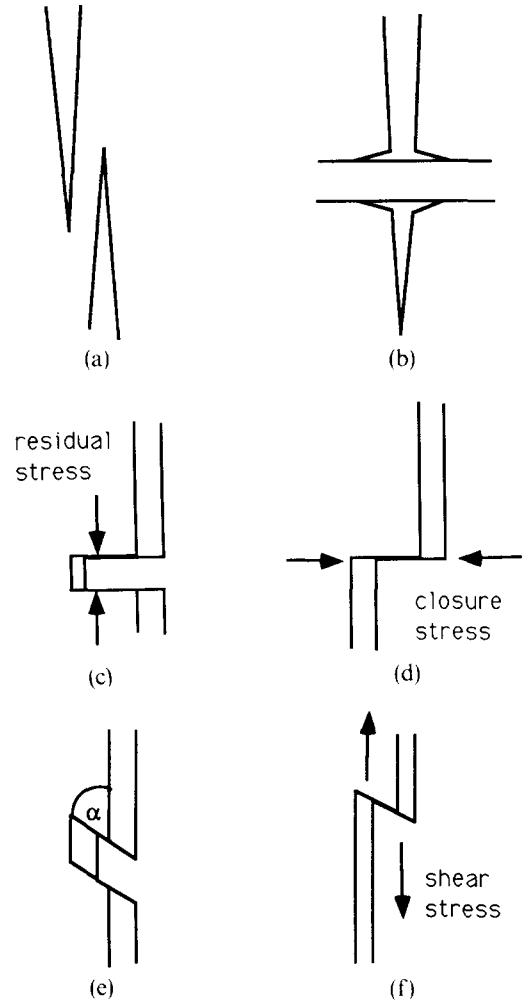

Fig. 15. Schematic for possible bridge configurations: (a) and (b) intact (elastic) bridges with (a) no further debonding and (b) further debonding; (c) and (d) frictionally sliding (plastic) bridges with different geometries; (e) and (f) mechanically interlocked (elastic–plastic) bridges.

the crack direction (residual stresses or locally as well as externally applied shear stresses—Fig. 15(c) and (d)) to stresses perpendicular to the crack direction (closure stresses). They store elastic energy in accordance with the locally applied closure stress p and the crack opening $2u$. While the crack opening increases, this elastic energy is, however, continuously dissipated. Accordingly, the $p(u)$ function is continuously decreasing. Frictionally sliding bridges can fail catastrophically or simply slide out of their respective sockets until no surface contact remains. Crack interface tractions can be active in regions with CODs $> 1\,\mu$m and therefore might be to a large degree responsible for long crack R-curve behaviour.

Frictionally sliding bridges are, however, difficult to characterize, since it is unclear whether crack interfaces are locally in frictional contact or only form a narrow gap. Subsidiary elements, like secondary cracks (Fig. 9) or subsequent performance

(debris accumulation during cyclic fatigue[17]) or crack redirection (Fig. 8), are therefore helpful indicators of their true existence. Deformation, since energy has been dissipated, is essentially permanent. In analogy to elastic bridges, therefore, frictionally sliding bridges are considered to be synonymous with plastic bridges. This implies strong susceptibility to cyclic fatigue.[17]

Mechanical interlocking appears to occur preferably in microstructures containing platelets or acicular elements and, for example, could not occur in a hexagonal network. It usually relies on intergranular fracture. Failure of this type of restraining element occurs mostly through fracture of the restraining matrix (see Figs 9 and 13), grain rotation (Fig. 8) or possibly fracture of the reinforcement. In cases where the angle α (Fig. 15(e) and (f)) is close to 90° complete pull-out (Fig. 12) might occur.

In contrast to the frictionally sliding bridge, residual stresses or shear stresses are not required to create a closure stress. On the contrary, pull-out of a misaligned element can generate a local shear stress (Fig. 15(c)). The absorbed energy is to an increasing degree stored elastically (in the reinforcement and restraining matrix) but also dissipated during frictional sliding. The elastically stored energy may build up until fracture of the restraining matrix occurs, where the $p(u)$ function will drop to zero. Mechanically interlocked bridges are therefore termed synonymous with elastic–plastic bridges and can be seen as an intermediate form of the two other categories. The part of the elastic–plastic restraining element which relies on a component of friction is succeptible to mechanical fatigue.

A distinction between the three bridging elements can be somewhat diffuse or their behaviour can be mixed. Frictionally sliding bridges with small misalignment can turn into mechanically interlocked bridges where the energy is then stored, to a large degree, elastically. One bridge type can also fail and thereby transform into another type, as Fig. 3 proves, where the elastic bridge turns into a frictionally sliding bridge. In general, depending on the misalignment angle α, an elastic bridge can (but need not) turn into a plastic or elastic–plastic bridge. Synergistic processes can be observed, as in Fig. 9, where a mechanically interlocked bridge at P creates a local mode II, which pins the frictionally sliding bridge at S.

At this juncture an attempt is made to clarify a point which caused confusion in several discussions leading to this work. The fact that all the energy once stored in the restraining elements is finally lost in an irreversible manner may lead to the conclusion that the R-curve is continuously and forever rising, since ever more energy is required to drive the crack with increasing crack length. The crack resistance at steady state, however, is at its peak value. The energy to drive the crack further indeed has to be increased (increasing load displacement); the energy absorbed per increment of crack advancement, however, remains constant, once the steady-state bridging zone is reached. Energy is continuously absorbed by the restraining elements as well as by the crack tip region to create new surface energy. Were this not the case, the crack would advance with constant velocity in a constant K-specimen under constant load (no further energy input).

5.2 Formation of crack closure forces

The discussion on bridge formation has been based solely on the discussion of the opening of a suitably positioned microcrack source in front of the crack tip. While this mechanism is based on microscopical in-situ observation, it nevertheless forms a restriction. A microcrack, as it appears on the surface, might be connected to the primary crack subsurface. Also bridge formation during continuous crack propagation will have to be described by a different model. However, the same ideas based on T_0, σ_R, etc., will be raised. In reviewing the separate points leading to bridge formation the following should be noted.

A variation in grain size and grain shape had not been discussed before as leading to bridge formation; the dependence of closure stress (bridge performance, not bridge formation) on grain size and grain shape had been established for the case of alumina by Bennison & Lawn.[9] Both parameters (besides σ_{res}) are essential in the description of microcrack formation and give a microcrack zone size, depending on grain facet size and shape.[20] The beneficial effect of a slight degree of inhomogeneity has been realized with the Al_2TiO_5/Al_2O_3 composite.[14] The rather strong R-curve of somewhat heterogeneous commercial aluminas[17] might also be rationalized under this aspect.

There are no recipes for adjusting the grain boundary toughness. In fact this parameter is the one which is clearly most difficult to work with from the ones mentioned. A partial reduction in T_0 at selected grain facets would enhance bridge formation but also reduce the average grain boundary toughness of the material, thereby reducing the base level of the crack resistance from where an R-curve could be built. Materials with non-cubic crystallographic structure (e.g. α-SiC; see Fig. 1) and an

anisotropy in fracture energies are thought to be candidates for the formation of elastic bridges (aided by local mode II, III; see Figs 1–3).

Local adjustment of residual stresses has been proven to be effective[13,14,28] in terms of producing materials with strong *R*-curves. This approach might lead to the formation of large elastic bridges, mechanically interlocking and frictionally sliding elements. It can bring a synergistic effect with microcrack toughening, but excessive residual stress might lead to microcrack growth and coalescence, rendering the material susceptible to environmentally influenced static fatigue.

A stress field asymmetry arises where either an external mode II is applied (trivial) or the bridging zone (e.g. through mechanical interlocking) creates a mode II at the crack tip or the crack tip senses a difference in Young's moduli. In the latter case the crack prefers to extend into the lower modulus material[29] and will drive towards a mode $II = 0$ condition and therefore a deviation from the straight crack path. A difference of Young's moduli has been demonstrated effective in that sense in experiments where pores ($E = 0$) were shown to cause a crack deviation towards the pore[30] (lower modulus phase). Distortion of the crack tip stress field has been discussed by Swanson[15] and can be related to resultant fracture surface markings. It is also well known that a combined mode I–mode II (or III) loading leads to increased fracture energy both at interfaces[31] and monoliths.[32] Quantitative statements of mixed-mode stress-induced disruption of the crack plane due to either tractions in the bridging zone or microstructural variation in front of the crack tip are not yet available.

In establishing eqn (1) it was remarked that the model for generation of a microcrack zone is closely related to the present approach. With this in mind it comes as no surprise that microcrack toughening and bridge formation are related phenomena and rely—in part—on adjusting the same set of microstructural parameters. Materials which show microcrack toughening might therefore also be prone to showing bridge formation. In other words, in searching for new materials which provide good toughening through crack bridging, materials which exhibit microcracking might be good candidates (the reverse is not necessarily true, since bridge formation does not rely solely on residual stresses). In this context the discussion over the last years, whether microcrack toughening or crack bridging is the dominant mechanism in a given material, appears in a different light. Both processes can be seen as related where the formation is concerned, with one process the extreme form of a common parent. The parent in this case is the formation of a microcrack in front of the crack tip, which subsequently links up to the primary crack or does not. While this might be a somewhat over-simplistic view, considering the assumptions made during the discussion on crack formation, it might help to bring the proponents for both mechanisms closer together.

It should be emphasized that bridge formation should not be confused with bridge performance or with the prediction of actual closure forces. In considering the closure stress obtainable in a given material, both processes, bridge formation (leading to a parameter for the bridge density) and actual closure stress of a given singular bridging element, have to be combined to give the average smeared-out closure stress for a given crack–microstructure system.

6 Conclusions

A classification scheme for crack bridging elements in brittle solids is proposed, based on appearance and deformation behaviour. The three types are:

(A) Intact (or elastic) bridges, which
- —store an increasing amount of elastic energy with increasing crack opening;
- —are represented by an increasing $p(u)$ function;
- —fail catastrophically under release of acoustic energy, thereby possibly turning into a bridge of one of the two other categories;
- —are—by definition of their reversible nature—resistant to cyclic loading.

(B) Frictionally sliding (or plastic) bridges, which
- —continuously dissipate energy, which is stored elastically, with increasing crack opening;
- —are represented by a decreasing $p(u)$ function;
- —rely on an element of friction to transform a clamping or shear stress into a closure stress;
- —can fail catastrophically or simply slide out of their respective sockets;
- —are susceptible to cyclic loading.

(C) Mechanically interlocked (or elastic–plastic) bridges, which
- —combine an element of storing elastic energy with a mechanism of continued dissipation of frictional energy;
- —are represented by a $p(u)$ function which strongly depends on the inclination angle α;
- —can fail through fracture of the restraining

matrix, bridging element or rotation of the reinforcing component;
—are to a certain degree susceptible to cyclic loading.

Bridge formation has been related to the formation of a microcrack ahead of the crack tip, an event which has been observed repeatedly. The parameters influencing bridge formation are grain size and shape, crack resistance of a grain boundary or an intergranular fracture plane, residual stresses and stress field asymmetry at the crack tip, the latter derived from both a difference of Young's moduli of different phases ahead of the crack as well as from tractions in the bridging zone. Very simply, small (not excessive) degrees of heterogeneity, anisotropy in interfacial fracture energies, thermal expansion anisotropy leading to residual stresses (or phases with different thermal expansion coefficient) and/or different Young's moduli are expected to increase bridge formation.

Acknowledgements

For either help in sample preparation or many fruitful discussions the author is indebted to Steve Bennison, Linda Braun, Nils Claussen, Ed Fuller, Rolf Janssen, Ralph Krause, Srinivasarao Lathabai, Brian Lawn and Manfred Sindel. The experimental part of this work was supported by the US Air Force, Office of Scientific Research. The theoretical part of this study was supported by the Volkswagen Foundation under Contract Number I/66 790.

References

1. McMeeking, R. M. & Evans, A. G., Mechanics of transformation toughening in brittle materials. *J. Am. Ceram. Soc.*, **65** (1982) 242–6.
2. Rühle, M., Evans, A. G., McMeeking, R. M., Charalambrides, P. G. & Hutchinson, J. W., Microcrack toughening in alumina/zirconia. *Acta metall.*, **35** (1987) 2701–10.
3. Hübner, H. & Jillek, W., Sub-critical crack extension and crack resistance in polycrystalline alumina. *J. Mat. Sci.*, **12** (1977) 117–25.
4. Knehans, R. & Steinbrech, R., Memory effect of crack resistance during slow crack growth in notched Al_2O_3 bend specimens. *J. Mat. Sci. Lett.*, **1** (1982) 327–9.
5. Swanson, P. L., Fairbanks, C. J., Lawn, B. R., Mai, Y.-W. & Hockey, B. J., Crack-interface grain bridging as a fracture resistance mechanism in ceramics. I: Experimental study on alumina. *J. Am. Ceram. Soc.*, **70** (1987) 279–89.
6. Becher, P. F., Microstructural design of toughened ceramics. *J. Am. Ceram. Soc.*, **74** (1991) 255–69.
7. Smith, E., Estimating the toughening effect of crack-bridging particles in a brittle matrix. *Int. J. Fract.*, **45** (1990) 283–98.
8. Budiansky, B., Hutchinson, J. W. & Evans, A. G., Matrix fracture in fiber-reinforced ceramics. *J. Mech. Phys. Solids*, **34** (1986) 167–89.
9. Bennison, S. J. & Lawn, B. R., Role of interfacial grain-bridging sliding friction in the crack-resistance and strength properties of nontransforming ceramics. *Acta metall.*, **37** (1989) 2659–71.
10. Rödel, J., Kelly, J. F. & Lawn, B. R., In-situ measurements of bridged crack interfaces in the scanning electron microscope. *J. Am. Ceram. Soc.*, **73** (1990) 3313–18.
11. Rödel, J., Kelly, J. F., Stoudt, M. R. & Bennison, S. J., A loading device for fracture testing of compact tension specimen in the SEM. *Scanning Microscopy*, **5** (1991) 29–35.
12. Frei, H. & Grathwohl, G., Development of a piezo-translator-based bending device for in-situ SEM investigations of high performance ceramics. *J. Phys. E.*, **22** (1989) 589–93.
13. Runyan, J. L. & Bennison, S. J., Fabrication of flaw-tolerant aluminum titanate-reinforced alumina. *J. Eur. Ceram. Soc.*, **7** (1991) 93–9.
14. Padture, N. P., Bennison, S. J., Runyan, J. L., Rödel, J., Chan, H. M. & Lawn, B. R., Flaw tolerant Al_2O_3–Al_2TiO_4 composites. In *Ceramic Transactions, Vol. 19: Advanced Composite Materials*, ed. M. D. Sacks. American Ceramic Society, Westerville, OH, 1991, pp. 715–21.
15. Swanson, P. L., Crack-interface traction: a fracture-resistance mechanism in brittle polycrystals. In *Advances in Ceramics, Vol. 22: Fractography of Glasses and Ceramics*, ed. V. D. Frechette. American Ceramic Society, Westerville, OH, 1988, 135–55.
16. Lawn, B. R. & Wilshaw, T. R., *Fracture of Brittle Solids*. Cambridge University Press, London, 1975, pp. 46–73.
17. Lathabai, S., Rödel, J. & Lawn, B. R., Cyclic fatigue from frictional degradation at bridging grains in alumina. *J. Am. Ceram. Soc.*, **74** (1991) 1340–48.
18. Rödel, J., Fuller, E. R. Jr. & Lawn, B. R., In-situ observations of toughening processes in alumina reinforced with silicon carbide whiskers. *J. Am. Ceram. Soc.*, **74** (1991) 3154–7.
19. Fu, Y. & Evans, A. G., Microcrack zone formation in single phase polycrystals. *Acta metall.*, **30** (1982) 1619–25.
20. Lawn, B. R., Fundamental condition for existence of microcrack clouds in monophase ceramics. *J. Eur. Ceram. Soc.*, **7** (1991) 17–20.
21. Sih, G. C., *Handbook of Stress Intensity Factors*. Lehigh University Press, Bethlehem, PA, 1973.
22. Tvergaard, V. & Hutchinson, J. W., Microcracking in ceramics induced by thermal expansion or elastic anisotropy. *J. Am. Ceram. Soc.*, **71** (1988) 157–66.
23. Atkins, A. G. & Mai, Y.-W., *Elastic and Plastic Fracture*. John Wiley & Sons, New York, 1985, pp. 198–219.
24. Venkinis, G., Ashby, M. F. & Beaumont, P. W. R., *R*-Curve behaviour of Al_2O_3 ceramics. *Acta metall. mater.*, **38** (1990) 1151–62.
25. Rose, L. R. F., Crack reinforcement by distributed springs. *J. Mech. Phys. Solids*, **35** (1987) 383–405.
26. Rühle, M., Dalgleish, B. J. & Evans, A. G., On the toughening of ceramics by whiskers. *Scripta Met.*, **21** (1987) 681–6.
27. Knehans, R. & Steinbrech, R., Effect of grain size on the crack resistance curves of Al_2O_3 bend specimens. *Sci. Ceram.*, **12** (1983) 613–19.
28. Lutz, E. H., Claussen, N. & Swain, M. V., K^R-Curve behavior of duplex ceramics. *J. Am. Ceram. Soc.*, **74** (1991) 11–18.
29. Evans, A. G., Dalgleish, B. J., He, M. & Hutchinson, J. W., On crack path selection and the interface fracture energy in bimaterial systems. *Acta metall.*, **37** (1989) 3249–54.
30. Penugonda, M. R., Virkar, A. V. & Shetty, D. K., Prediction of crack paths in particulate composites using electrical analog. *J. Am. Ceram. Soc.*, **73** (1990) 340–5.
31. Cao, H. C. & Evans, A. G., An experimental study of the fracture resistance of bimaterial interface. *Mechanics of Materials*, **7** (1989) 295–305.
32. Suresh, S. & Tschegg, E. K., Combined mode I–mode III fracture of fatigue-precracked alumina. *J. Am. Ceram. Soc.*, **70** (1987) 726–33.